Published in final edited form as:
Mol Cancer Res. 2008 September ; 6(9): 1385. doi:10.1158/1541-7786.MCR-08-0094.

AUTOUBIQUITINATION OF BCA2 RING E3 LIGASE REGULATES ITS OWN STABILITY AND AFFECTS CELL MIGRATION

Yutaka Amemiya, **Peter Azmi**, and **Arun Seth**
Division of Molecular and Cellular Biology, Sunnybrook Research Institute, and Department of Laboratory Medicine and Pathobiology, University of Toronto, Toronto, Ontario, Canada

Abstract

Accumulating evidence suggests that ubiquitination plays a role in cancer by changing the function of key cellular proteins. Previously, we isolated BCA2 gene from a library enriched for breast tumor mRNAs. The BCA2 protein is a RING type E3 ubiquitin ligase and is overexpressed in human breast tumors. In order to deduce the biochemical and biological function of BCA2, we searched for BCA2 binding partners using human breast and fetal brain cDNA libraries and BacterioMatch two-hybrid system. We identified 62 interacting partners, majority of those were found to encode ubiquitin precursor proteins including ubiquitin C and ubiquitinA-52. Using several deletion and point mutants, we found that the BCA2 zinc finger (BZF) domain at the N-terminus specifically binds ubiquitin and ubiquitinated proteins. The autoubiquitination activity of BCA2, RING-H2 mutant, BZF mutant, and various lysine mutants of BCA2 were investigated. Our results indicate that the BCA2 protein is strongly ubiquitinated and no ubiquitination is detected with the BCA2 RING-H2 mutant, indicating that the RING domain is essential for autoubiquitination. Mutation of the K26 and K32 lysines in the BZF domain also abrogated autoubiquitination activity. Interestingly, mutation of the K232 and K260 lysines in and near the RING domain resulted in an increase in autoubiquitination activity. Additionally, in cellular migration assays, BCA2 mutants showed altered cell motility compared to wild-type BCA2. On the basis of these findings, we propose that BCA2 maybe an important factor regulating breast cancer cell migration/metastasis. We put-forward a novel model for BCA2 E3 ligase mediated cell regulation.

INTRODUCTION

The ubiquitin and ubiquitin-like pathways are integral to the normal function of eukaryotic cells (1-8). Protein turnover, trafficking, and the modulation of protein function have been ascribed to ubiquitination (9-11). Defects in ubiquitination programs have been described in the pathogenesis of several human diseases, including cancer.

Ubiquitination of target proteins proceeds in a stepwise format, involving E1, E2 and E3 enzymes. In the first step ubiquitin is activated in an ATP-dependent manner by the activating enzyme known as E1. In the second step, the activated ubiquitin is transferred to a conjugating enzyme denoted as E2. In the last step, the E2 enzyme interacts with a specific E3 ubiquitin-protein ligase resulting in the autoubiquitination of the E3 or ubiquitination of target proteins on specific lysine residues (reviewed extensively (12-14)). Target proteins can be ubiquitinated in a manner that alters their function, localization or stability within the cell. Generally, the addition of one to four ubiquitin molecules to a target protein leads to a change in its localization

Address Correspondence to: Arun Seth, Ph. D., Department of Molecular and Cellular Biology, Sunnybrook Research Institute, 2075 Bayview Ave. Rm. 238, Toronto ON, M4N 3M5, Canada., Tel. 416-480-6100 ext. 7897, Fax. 416-480-5737, E-mail: arun.seth@utoronto.ca.

and/or function. The addition of many ubiquitin moieties (poly-ubiquitination) leads to protein degradation by the 26S proteasome. Specificity in targeting proteins for ubiquitination lies mostly in the E3 enzyme. There are two major classes of E3 enzymes, the first being the HECT-type E3 ubiquitin ligases (15). These include Smurf1, Smurf2, AIP4, and Nedd4 among others. The second class of E3 enzymes is the RING finger domain proteins. For example, ring finger proteins Mdm2, Efp and BRCA1/BARD, have ubiquitin E3 ligase activity and have been shown to have a significant biological role in breast and other cancers (1,13,16,17). A notable feature of RING E3 ubiquitin ligases is that the enzymatic activity of the E3 ligase can be monitored through autoubiquitination of the protein in-vitro. Autoubiquitination is the process by which the E3 enzymes catalyze the addition of poly-ubiquitin to themselves. This can result in the degradation or change of function of the E3 protein *in vivo.*

We identified BCA2, a RING finger protein that is over-expressed in more than 50% of invasive breast cancers compared to normal tissues and can be linked to breast cancer cell proliferation in vitro (16,18). Overexpression of BCA2 increases proliferation of NIH3T3 fibroblasts, whereas small interfering RNA inhibits growth of BCA2-expressing breast cancer cells. BCA2 is expressed in the nucleus and cytoplasm of breast cancer cells, suggesting multiple functions (16). The BCA2 protein possesses autoubiquitination activity, which depends on its RING domain. Though it is well accepted that E3 enzymes can play an integral role in the oncogenic process (16,19,20), it is less well understood how deregulation of an E3 may occur.

To gain a better understanding of how RING E3 enzymes mediate target identification and ubiquitination, we investigated the molecular mechanisms that regulate BCA2 E3 ligase activity. The BCA2 protein contains 304 amino acids and the protein sequence is conserved in various species (mouse, fruit fly, sea urchin and fission yeast)(16). Highly conserved regions include the Zn-finger domain and the RING-H2 finger, suggesting important functions for these domains (Fig. 1A). Other regulatory motifs include a consensus AKT phosphorylation site and we have shown that BCA2 protein can be phosphorylated by AKT (21). We demonstrated that BCA2 has E3 ligase activity by exhibiting its ability to undergo autoubiquitination *in vitro* using bacterially expressed recombinant protein. Like other E3 ubiquitin ligases, the ubiquitination activity of BCA2 is abolished by mutation of two essential zinc-coordinating cysteine residues in the RING domain (16). A closely related protein, RNF126 has also been cloned and shares 46% indentity with BCA2. We have shown that RNF126 also possesses autoubiquitination activity (22).

Our laboratory and others have shown that BCA2 binds to Rab7, a member of the Rab family of small G proteins that regulate intracellular vesicle traffic, including exocytosis and endocytosis (22,23). Interestingly, there is some evidence that overexpression of BCA2 may down-regulate the epidermal growth factor receptor (23). We and others have found that Rab7 is not a substrate for BCA2 ligase activity (data not shown, 24). Therefore, we sought BCA2 binding partners using the BacterioMatch system and human breast and fetal brain cDNA libraries. Interestingly, the majority of the positive clones were found to encode ubiquitin precursor genes including ubiquitin C and ubiquitinA-52 suggesting that BCA2 also binds non-covalently to ubiquitin, and/or ubiquitin-modified proteins. Using various deletion and point mutants of BCA2, we identified a novel ubiquitin interacting domain in the BCA2 protein and the major lysine residues required for the autoubiquitination activity. Furthermore, we show that alteration in the autoubiquitination activity of the BCA2 protein affects both the protein's steady state levels and BCA2 mediated cellular function. On the basis of our findings we propose a novel mechanism for BCA2 E3 ubiquitin ligase activity and its role in cell regulation.

RESULTS

Characterization of BCA2 partner proteins

To isolate BCA2 binding partners we used the BacterioMatch II system and the human breast and fetal brain cDNA libraries. Three million clones were screened and 62 were found to be strongly positive after tertiary screening. Interestingly, all of the sixty-one genes encode proteins that function within in the ubiquitin-proteasome pathway. Fifty of the positive clones encoded ubiquitin C, ten of them the ubiquitin A-52 ribosomal fusion protein (Uba52) and one clone corresponded to Ubc9 (Fig. 1B). To confirm the interaction between ubiquitin and BCA2, we used various lengths of concatomerized ubiquitin moities (Ub_1 to Ub_6) fused to recombinant GST in a pull down assay with recombinant BCA2 protein. We show that the BCA2 protein specifically binds to all GST-tagged ubiquitin fusion proteins, but not to GST alone (Fig. 1C). Notably, strongest binding was observed with the Ub_6 ubiquitin, which contains six tandem repeats of the ubiquitin protein.

Identification of a novel ubiquitin interacting domain in BCA2

Towards the N-terminal region of the protein (residues 22-41), BCA2 contains a single zinc finger (CxxC--CxxC). We have termed BCA2 zinc finger domain as BZF. At least four other zinc finger domains PAZ, NZF, UBZ and A20 have been shown to interact with ubiquitin (Fig. 2A)(25-30). We hypothesized that the BCA2 zinc finger may also interact with ubiquitin. To test this hypothesis, we tested several BCA2 deletion variants in a directed bacterial two-hybrid assay (Fig. 2B). Results in Figure 2C show that only the wild type BCA2 and the N-terminal fragment mutant that retain the complete BZF domain resulted in colony growth, but not with internal or c-terminal fragment mutant indicating that the interaction of BCA2 with Ubiquitin C or Uba52 requires the BZF domain.

To further confirm that the BCA2 BZF domain is indeed a functional uniquitin-binding motif, we employed a modified pull-down approach where we utilized wild type or site directed BZF domain mutant of BCA2 in which cysteine residues of the BZF zinc finger were substituted with alanines (Fig. 2D). RING domain, and AKT site point mutants were used as controls (Fig. 2D). Using ubiquitin-conjugated beads, we demonstrated that wild type BCA2 and only the mutants that retained wild type-BZF domain interact with ubiquitin (Fig. 2E).

Quantification of BZF binding affinity for ubiquitin

To better understand the binding affinity of the BZF domain for ubiquitin, we conducted a quantitative association study to determine the Kd for this interaction. Surface Plasmon Resonance (SPR) biosensors analyze macromolecular interactions in real-time without the need to label the substrates. To quantify the BCA2-ubiquitin interactions by SPR, a layer of BCA2 was adsorbed onto the surface of the sensor chip and a solution of ubiquitin was subsequently flowed over the surface-bound BCA2 for binding. As a control we used the zinc ejecting compound, disulfiram, which we have shown to disrupt the BZF domain (16). When the BZF domain is disrupted, either through zinc ejection by disulfiram or by specific mutation of cysteine to alanine in the BCA2 zinc finger (BZF mutant), we observed a loss of ubiquitin binding to BCA2. We found that the BZF domain binds ubiquitin with a Kd of 29.6 (+/-3.2) μM (Fig. 3A) and shows a much higher affinity when compared to other known ubiquitin binding domains (Fig. 3B).

Autoubiquitination activity of BCA2 is dependent on its RING domain

Autoubiquitination is a characteristic of RING E3 ligases (31,32) and in the absence of a specific target, autoubiquitination can be used to monitor E3 enzymatic activity. Furthermore, autoubiquitination may represent a significant means by which E3 ligases auto-regulate their

own stability within the cell. It is therefore important to understand the mechanisms by which autoubiquitination occurs. E3 autoubiquitination can be evaluated in an *in vitro* autoubiquitination assay, where the E3 is mixed with its cognate E2 and the other factors required for the ubiquitination reaction.

The actual E2 enzymes that BCA2 coordinates with for autoubiquitination are UbcH5s. Using either UbcH5 a, b or c, we evaluated BCA2 auto-ubiquitination activity through an in vitro ubiquitination assay. We showed that wild type BCA2 is autoubiquitinated in the presence of UbcH5b however in the absence of a cognate E2, BCA2 lacks autoubiquitination activity (Fig. 4). Like other RING E3 ligases, the enzymatic activity responsible for BCA2 autoubiquitination requires intact RING finger domain. Because BCA2 losses its autoubiquitination activity when the cysteines C228 and C231 within the RING finger are mutated indicating that the first two cysteine residues in the RING-finger domain are necessary for E3 ligase activity. However, the AKT phosphorylation site mutant displayed modest autoubiquitination activity.

Kinetics of BCA2 autoubiquitination

The effects of various BCA2 mutants on autoubiquitination kinetics were examined in time-course autoubiquitination assays. Aliquots of *in vitro* reactions after 15, 30, 60 and 90 minutes were immunoblotted to reveal ubiquitinated BCA2 protein (Fig. 5). Densitometry values normalized to background were plotted and graphed for each BCA2 variant tested (Fig. 6). Wild type BCA2 produced detectable ubiquitination after 60 minutes, increasing after 90 minutes (Fig. 5A and Fig.6, orange square). No effect was observed when we used the AKT site mutant of BCA2 (Fig. 5B and Fig.6 purple triangle). In contrast, mutation of essential cysteines in the BZF domain increased the amount of ubiquitinated BCA2 protein after 60 and 90 minutes (Fig. 5C and Fig.6, dark blue square). As we have shown above and in (16) that the ubiquitination activity is completely abolished by mutation of the RING domain (Fig. 5D and Fig.6, green triangle).

Mutation of lysine and cysteine residues affect autoubiquitination of BCA2

Ubiquitination occurs on lysine residues. BCA2 possesses six lysine residues that are located almost in pairs at the N-terminal, middle and C-terminal regions of the protein. To elucidate which lysine residues are responsible for autoubiquitination, we created arginine mutants of all six BCA2 lysines. The two N-terminal lysines are located in the BZF domain and we denote these two residues as the N-terminal lysines (K26 and K32). The next two lysines are located between the AKT phosphorylation site and the RING finger domain and we denote these two residues as the internal lysines (K206 and K208). The last two lysines are located within and just next to the RING finger domain. We denote these last two residues as the C-terminal lysines (K232 and K260) (Fig.1A).

In an autoubiquitination time-course assay, mutation of the N-terminal lysines (K26R and K32R) located within the BZF region resulted in a complete lack of ubiquitinated BCA2, indicating that these are the most likely sites of BCA2 autoubiquitination (Fig. 5E and Fig.6, orange square). However individual mutations of the N-terminal lysines produced ubiquitinated BCA2, indicating that either of these lysines (K26R and K32R) can be used for autoubiquitination (Fig. 5F and Fig.6, red triangle and Fig. 5G and Fig.6, green triangle). Mutation of the internal lysines (K206R/K208R) produced autoubiquitinated BCA2 protein after 60 minutes (Fig. 5H and Fig.6, blue triangle). Interestingly, mutation of the two C-terminal lysines (K232R/K260R) located within and nearby the RING domain increased both the amount and the kinetics of BCA2 ubiquitination reaction (Fig. 5I and Fig.6, purple square). Further refinement of this observation was done using single C-terminal lysine mutants of BCA2. Mutation of C-terminal lysine K232 showed a slight decrease in autoubiquitination

compared to wild type BCA2 (Fig. 5J and Fig.6, dark blue triangle). BCA2 autoubquitination was greatly enhanced by mutation of the C-terminal lysine K260R (Fig. 5K and Fig.6, blue square). Lastly, we combined mutations that resulted in an increase in BCA2 autoubiquitination, namely the BZF and C-terminal lysine mutants. Here we observed further increase in BCA2 autoubiquitination (Fig. 5L and Fig.6, red square). As a result, it appears that disruption of the BCA2 BZF domain or C-terminal K260 lysine increases both the amount and the rate of BCA2 autoubiquitination.

From the kinetic analysis we were able to subdivide different BCA2 variants into four groups; ligase dead, ligase normal, ligase high and ligase very high (Fig. 6).

BCA2 autoubiquitination activity correlates with its own stability

Recently, we had shown that BCA2 steady state protein levels could be stabilized by addition of the proteasome inhibitor MG-132 (16). This work also demonstrated that mutation of the RING domain prevented proteasomal degradation of the BCA2 protein, indicating a possible autoubiquiniation mediated auto-regulation mechanism for the BCA2 protein. In this study, we compared the steady state levels of wild type, lysine mutants, BZF domain mutants, and RING mutants of BCA2 in HEK293T cells (Fig. 7). Mutation of the BZF domain cysteines and mutation of the C-terminal lysines (K232R/K260R) located within and nearby the RING domain resulted in decreased amounts of BCA2 protein relative to wild type protein (Fig. 7 lanes 7 and 11 vs. lane 1). Since mutation of lysines within and near the RING domain reduces BCA2 stability, this indicates that these mutations do not affect the function of the RING domain but do increase the rate of BCA2 protein degradation. This occurred in both the absence and the presence of the proteasome inhibitor MG-132 (Fig. 7 lanes 7 and 8), suggesting that autoubiquitination and degradation of BCA2 is markedly enhanced by mutations of the BZF domain and the C-terminal lysines. As expected, autoubiquitination-deficient N-terminal lysine mutants and RING finger mutant did not show an increase in BCA2 degradation which is in agreement with our ubiquitination studies. Our observations indicate that the BCA2 RING is required for BCA2 autoubiquitination and that the two N-terminal lysines are the most likely sites for polyubiquitination of the BCA2 protein.

Enhanced BCA2 E3 ligase activity is associated with an increase in cellular motility in MCF7 breast cancer cells

To better understand the role of BCA2 in cell migration, we generated various BCA2 and its variants expressing MCF-7 cell-lines. The expression of exogenous BCA2 protein in these cell-lines was examined by in situ immunofluorescence (Fig. 8) and Western blotting assays (Fig. 9A). Immunofluorescence was carried out as described in Material and Methods. The wild-type BCA2 protein showed diffused expression throughout the cell with small areas of intense staining (Fig. 8A), the RING mutant showed similar pattern as wt BCA2 however it was expressed at much higher levels (Fig. 8D). The N-terminal lysine mutant showed punctate staining in the cytoplasm and near the cell membrane (Fig. 8B). A similar speckled expression pattern was observed for the C-terminal lysine mutant and the BZF mutant (Fig. 8C and E). We determined the expression levels by Western blotting also and found that the proteins of the autoubiquitination-dead versions of BCA2 (RING and N-terminal lysine mutants) were stabilized and expressed at a higher level than the wild type BCA2 protein. On the other hand, the BZF and C-terminal lysine mutants, which have very high autoubiquitination activity, appeared at lower levels than the wild type BCA2 protein (Fig. 9A).

The scratch wound assay was used to assess the effects of BCA2 and its mutants on the cellular migration associated with wound closing. MCF-7 cells stably expressing different BCA2 variants were plated to confluence in a 6-well plate. A single scratch wound was created in each well using the pipette tip, and cells were treated with hydroxyurea to block cellular

proliferation. The wound area within each well was imaged at fixed time intervals (Fig. 9B). We quantified the net migration of BCA2 expressing MCF7 cells using three independent points in each experiment utilizing imaging software (see Materials and Methods) and the data is plotted as bar graphs (Fig. 9C). We discovered that the MCF-7 cells expressing the wild type BCA2 protein were significantly more motile than control cells. The BZF domain mutant showed the most migration of all the MCF-7 BCA2 expressing stable lines tested, the wound was 75% closed at 24hr time point and completely closed after 48hours. In contrast, mutants that abolished autoubiquitination (RING mutation, or N-terminal lysine mutations) showed decreased mobility and less than 20% wound closure was seen after 24 hours.

DISCUSSION

RING E3 ligases play pivotal roles in protein degradation and receptor mediated endocytosis. BCA2 is a RING finger protein possessing ubiquitination ligase activity (16). Originally isolated by us through subtractive hybridization cloning from breast cancer cells, we later demonstrated that BCA2 is over-expressed in invasive breast cancers and is a potential target for therapeutic interventions (16,18,33). BCA2 E3 ligase is co-regulated with estrogen receptor and plays a role in the regulation of epidermal growth factor receptor trafficking. The biological significance of BCA2 overexpression also lies in the area of cellular transformation, as ectopic BCA2 increased breast cancer cell line proliferation and siRNA inhibited the growth of cultured cells (16). The mechanism for these effects likely lies in its intrinsic ubiquitination activity (16). This was further illustrated when we examined stably expressing MCF-7 cell lines of BCA2 and various BCA2 mutants. We showed that overexpression of BCA2 or BCA2 mutants that have an increase in autoubiquitination activity, also show an increase in cell migration when tested in scratch assays (Fig. 9).

The autoubiquitination activity requires the presence of an E2 as we demonstrated with UbcH5s (Fig. 4). We demonstrated that not all UBCs coordinate with BCA2, as autoubiquitination is not detectable when UBC3 is used in the assays (data not shown). The autoubiquitination activity of BCA2 also depends upon the RING domain, as BCA2 with a mutated RING domain lacking key cysteines is not ubiquitinated in vitro (Fig. 5) and only shows extremely low levels of ubiquitination in vivo (Fig. 4). We believe that the very low levels of BCA2 RING mutant autoubiquitination detected in vivo could be due to the presence of endogenous factors that might cooperate with BCA2 autoubiquitination activity. It is also possible that the ring mutant has residual autoubiquitination activity that is detectable only when the BCA2 is expressed in mammalian system”. . In this study we have also identified a novel zinc finger domain in BCA2, which is responsible for binding ubiquitin non-covalently. We termed this new domain as the BCA2 Zinc Finger (BZF) and provided evidence for the function of the BZF domain in the regulation of BCA2 autoubiquitnation activity (Fig. 5).

In order to identify targets of ubiquitination by BCA2, we identified BCA2 partner proteins using the BacterioMatch two-hybrid assay system (Fig. 1B). The specific targets included ubiquitin, ubiquitinated proteins and Ubc9. The interaction between these proteins and BCA2 was confirmed in a directed two-hybrid assay and Western blotting of immunocomplexes. Using mutants of BCA2, we confirmed that ubiquitin bound BCA2 in the BZF domain. The non-covalent interaction between ubiquitin and BCA2 suggests that the BCA2 ubiquitin ligase activity might be directed to other proteins in addition to itself. Owing to its activity as an E3 ubiquitin ligase and our understanding of the essential role of the ubiquitin proteasome system in protein homeostasis, BCA2 might influence tumorigenesis through regulation of cancer related proteins. BCA2 autoubiquitination appears to be a tightly controlled process, for we found that overexpression of hyperactive autoubiquitination mutants (K232R/K260R) in HEK293T cells resulted in almost complete absence of the BCA2 protein (Fig. 7). Point mutations that negatively affect BCA2 autoubiquitination activity such as the RING domain

mutant (which is catalytically dead) or the N-terminal lysine mutant (which can not receive poly-ubiquitination) result in accumulation of the BCA2 protein (Fig. 7). This observation indicates that BCA2 undergoes a self-regulated lifespan within the cell. The analysis of lysine mutants in BCA2 allowed us to find the sites of autoubiquitination, and to better understand novel mechanisms by which BCA2 may regulate target specificity. We found that the lysines contained within the BZF domain were required for BCA2 autoubiquitination. Furthermore, cysteine to alanine mutation of the BZF domain, which disrupts the zinc finger, led to an increase in autoubiquitination. This observation may indicate a mechanism whereby the BCA2 protein binds mono-ubiquitinated substrates via the BZF domain for further ubiquitination or for intracellular trafficking/targeting. However, when substrate levels drop or BCA2 levels are relatively high, BCA2 will autoubiqutinate itself, thereby regulating its levels according to substrate availability (Fig.10). Indeed, we observed strong differences in sub-cellular localization between the different mutants of BCA2, most notably the N-terminal lysine mutant and BZF mutant seem to have strong punctate patterns of expression compared to the wild-type BCA2 protein (Fig. 8). These results suggest that ubiquitination of BCA2 and the ubiquitin binding activity are important determinants for BCA2 stability and localization within the cell. This may represent a general mode of autonomous self-regulation for some of the E3 ligases.

MATERIALS AND METHODS

Antibodies

The mouse monoclonal anti-FLAG (M2), anti-glutathione-S-transferase (GST-2) and anti-β-actin (AC-15) antibodies were purchased from Sigma (St. Louis, MO). The monoclonal anti-polyhistidine (AD1.1.10) antibody was from R&D Systems (Minneapolis, MN). The monoclonal anti-ubiquitin (P4D1) antibody was from Cell Signaling Technologies (Beverly, MA). Horseradish peroxidase (HRP)-conjugated anti-mouse IgG secondary antibody was from Promega (Madison, WI).

Bacterial two-hybrid screening

A screen for BCA2 interacting proteins was performed using the BacterioMatch II Two-Hybrid System (Stratagene, La Jolla, CA). Full-length human BCA2 cDNA was cloned as a NotI-SalI fragment from FLAG-tagged pCMV-BCA2 (16) into the NotI-XhoI digested bait vector, pBT. The BacterioMatch human breast and fetal brain cDNA libraries constructed by pTRG vector were purchased from Stratagene. Cotransformants were screened by using medium lacking histidine and containing 5 mM 3-amino-1,2,4-triazole, as recommended by the manufacturer. The plates were incubated at 37°C for 24hrs and then at room temperature for 24hrs to detect weak interactors. Positive interactions were further confirmed by activation of the streptomycin resistance gene on selective plates. For negative controls, empty pBT and pTRG plasmids were co-transformed with pTRG library and pBT-BCA2, respectively. A positive control included the co-transformation of pBT-LGF2 and pTRG-Gal11, provided by Stratagene. DNA sequencing reactions of the respective inserts in pTRG vector were performed at the Sunnybrook Research Institute Genomic Core Facility. A BLAST search at the NCBI website was performed to identify proteins encoded by the respective cDNAs.

Expression vector constructs, and recombinant proteins

Histidine-tagged bacterial recombinant BCA2 and its mutant proteins were expressed in *E. coli* strain BL21 star (DE3) using pET100/D-TOPO expression vectors and purified on Ni-charged agarose beads as described (16). Point mutantions were generated in BCA2 coding region using the Quickchange site-directed Mutagenesis Kit from Stratagene. Ubiquitin (1, 2, 4, or 6 ubiquitin tandem repeats) cDNA were amplified from positive clones isolated from bacterial two-hybrid screening by PCR and inserted into the pGEX 4T3 expression vector (GE

Healthcare, Piscataway, NJ). Expressed GST-tagged ubiquitins were isolated from crude bacterial extract using Glutathione Sepharose 4B beads (GE healthcare, Piscataway, NJ).

BCA2 constructs for expression in mammalian cells

A vector expressing GST tagged BCA2 was created by inserting the BamHI fragment of BCA2 cDNA from FLAG-tagged pCMV-BCA2 into the pEBG-GST vector. Plasmids expressing His-BCA2 and mutants were constructed in the pEF1 vector from pET100-BCA2 and its mutants.

Cell Culture and transfection

HEK293T cells were maintained in high glucose DME medium (GIBCO) containing 10% fetal bovine serum without antibiotics at 37°C/5% CO_2. Cells were plated in 6-well plates the day before transfection was performed. Typically, four microgram vector DNA is transfected into cells by using the lipofectamine 2000 (invitrogen, Carlsbad, CA) and proteins are extracted 48 hours later as described (16).

Ubiquitination assays

Purified bacterially expressed His-BCA2 (100ng), or Flag-BCA2 immunoprecipitated with anti-FLAG mAb or GST-BCA2 pull-downed with Glutathione-Sepharose 4B (GE Healthcare, Piscataway, NJ) from 1mg of whole cell lysate of transfected HEK293T cells were analysed for autoubiquitination activity. BCA2 or its mutants were mixed with 3 μl of 10x reaction buffer (500mM Tris-HCl pH8.0, 20mM DTT and 50mM $MgCl_2$), 1 μl rabbit E1 (50 ng, Calbiochem, San Diego, CA), 1μl ubiquitin (1μg, Sigma), 1μl E2 (50 ng, UbcH5b bacterial product), 3μl 20mM ATP and water, to obtain a final reaction volume of 30μl. Each reaction mixture was incubated at 30°C for 90min, and proteins were visualized by Western blotting. Films were scanned on a Universal hood (SN75S) densitometer and signals quantitated using the Quantity One software (ver.4.3.1, Bio-Rad Laboratories, Segrate, Milan, Italy).

Analysis of protein stability

Four micrograms of wild type or mutant His-BCA2 vector DNA was transfected into HEK293T cells. After 40 hours, the proteasome inhibitor MG-132 (10 μmol/l) was added for a total of 8 hours. Control cells were treated with vehicle (DMSO) for 8 hours. Whole cell lysates were analyzed for protein expression levels by Western blotting.

Western blotting

Samples were mixed with 3x SDS-loading buffer containing 10% β-mercaptoethanol, boiled for 10 min. and loaded onto either 2% SDS-polyacrylamide gel or 4-20% Tris-HEPES-SDS polyacrylamide gel (PIERCE, Rockford, IL) for electrophoretic separation. The proteins were transferred on to a Hybond-P PVDF membrane (GE healthcare, Piscataway, NJ) at 15V overnight. All procedures after blotting were done at room temperature. The membrane was blocked for nonspecific binding with 5% milk powder in TBST (Tris buffered saline with 0.2% Tween-20), pH 7.4 for 1hr. Primary antibodies were diluted in blocking buffer and incubated for 2hr on a shaker. Membranes were then washed twice with TBST. Afterwards, each membrane was incubated with species-specific secondary antibody conjugated to horse radish peroxidase (HRP) enzyme for 1hr, washed three times with TBST and the signals were developed by the SuperSignal West Pico Chemiluminescent Substrate kit (PIERCE, Rockford, IL) and by exposure to X-ray film (Kodak, Rochester, NY).

SPR binding assay

Surface plasmon resonance measurements were performed on a BIACORE 3000 equipped with a research-grade CM5 sensor chip at 25C° with a flow rate of 50μl/min. Bacterially expressed and purified His-tagged BCA2 or zinc finger mutant (negative control) were immobilized at final densities of 0.8-1,0 kRU using traditional amine-coupling chemistry. Ubiquitin in running buffer (HBS-P) was injected in triplicate over the His-tagged BCA2 and zinc finger mutant surfaces at concentrations of 0, 7.81, 15.63, 31.25, 62.5, 125, 250, 500, 1000μM (50 sec at 50μl/min). Between subsequent injections of ubiquitin, surfaces were regenerated with an injection of HBS-P supplemented with 5mM DTT and 30μM $ZnCl_2$ for 6 min at 50μl/min. Binding responses were recorded and globally fit to simple 1:1binding models. The Structure of BZF domain was disrupted with an injection of 10μM disulfiram, the potent zinc-ejecting compound, for 10 min (16).

Immuno-Fluorescence

MCF7 clones stably expressing wild type or mutant BCA2 or empty vector were grown on glass cover slips for 24 hours. Cells were fixed with 4% PFA and blocked with 10% goat serum overnight at 4° C. Fixed and blocked cells were then probed with the monoclonal anti-polyhistidine (AD1.1.10) antibody (R&D Systems; Minneapolis, MN) for 8 hours at 4°C. Washes were done with PBS and repeated 3 times. Anti-mouse FITC-secondary fluorescent antibody was obtained from Sigma and used according to manufactures specifications. Cell nuclei were stained with DAPI. Final washes were done with PBS and repeated 5 times. Cover slips were mounted on slides and observed in a Zeiss Axiovert 200M system.

Wound healing assay

Individual MCF7 clones expressing wild type or mutant BCA2 were seeded in 6-well culture plates and grown to confluence forming a monolayer covering the surface of the entire well. After cells were serum-starved in serum-free DMEM for 18 h, the wound was created in the center of the cell monolayer by the gentle removal of the attached cells with a sterile plastic pipette tip. Debris was removed by PBS wash, and the cells received fresh DMEM medium with 10% FBS and 10mM Hydroxyurea. Four individual optical image of the wound edges were taken by the Zeiss Axiovert 200M microscope at 24h and 48h. The ability of the cells to migrate into the wound area was quantified by measuring the number of pixels in each wound closure area using Adobe Photoshop. Data are expressed as percentage wound closure from the initial wound area.

Acknowledgments

This work was supported in part by the Canadian Breast Cancer Research Alliance special program grant on metastasis and by NIH 1R01CA127258-01. We thank Drs. Daniel Dumont and Eric Yang of the SRI Proteomics Core Facility, for technical assistance and data analysis with Biacore 3000. We also thank Aiguo Zhang of SRI Genomic Core Facility for performing DNA sequencing of various BCA2 point mutants.

REFERENCES

1. Joazeiro CA, Weissman AM. RING finger proteins: mediators of ubiquitin ligase activity. Cell 2000;102:549–52. [PubMed: 11007473]
2. Tanaka K, Kawakami T, Tateishi K, Yashiroda H, Chiba T. Control of IkappaBalpha proteolysis by the ubiquitin-proteasome pathway. Biochimie 2001;83:351–56. [PubMed: 11295496]
3. Pan ZQ, Kentsis A, Dias DC, Yamoah K, Wu K. Nedd8 on cullin: building an expressway to protein destruction. Oncogene 2004;23:1985–97. [PubMed: 15021886]
4. Dohmen RJ. SUMO protein modification. Biochim Biophys Acta 2004;1695:113–31. [PubMed: 15571812]

5. Pickart CM, Eddins MJ. Ubiquitin: structures, functions, mechanisms. Biochim Biophys Acta 2004;1695:55–72. [PubMed: 15571809]
6. Aragon L. Sumoylation: a new wrestler in the DNA repair ring. Proc Natl Acad Sci USA 2005;102:4661–2. [PubMed: 15781853]
7. Mani A, Gelmann EP. The ubiquitin-proteasome pathway and its role in cancer. J Clin Oncol 2005;23:4776–89. [PubMed: 16034054]
8. Denison C, Kirkpatrick DS, Gygi SP. Proteomic insights into ubiquitin and ubiquitin-like proteins. Curr Opin Chem Biol 2005;9:69–75. [PubMed: 15701456]
9. Sawasdikosol S, Pratt JC, Meng W, Eck MJ, Burakoff SJ. Adapting to multiple personalities: Cbl is also a RING finger ubiquitin ligase. Biochim Biophys Acta 2000;1471:M1–12. [PubMed: 11004605]
10. Tyers M, Jorgensen P. Proteolysis and the cell cycle: with this RING I do thee destroy. Curr Opin Genet Dev 2000;10:54–64. [PubMed: 10679394]
11. Marmor MD, Yarden Y. Role of protein ubiquitylation in regulating endocytosis of receptor tyrosine kinases. Oncogene 2004;23:2057–70. [PubMed: 15021893]
12. Pickart CM. Mechanisms underlying ubiquitination. Annu Rev Biochem 2001;70:503–33. [PubMed: 11395416]
13. Burger AM, Seth AK. The ubiquitin-mediated protein degradation pathway in cancer: therapeutic implications. Eur J Cancer 2004;40:2217–29. [PubMed: 15454246]
14. Fang S, Weissman AM. A field guide to ubiquitylation. Cell Mol Life Sci 2004;61:1546–61. [PubMed: 15224180]
15. Ingham RJ, Gish G, Pawson T. The Nedd4 family of E3 ubiquitin ligases: functional diversity within a common modular architecture. Oncogene 2004;23:1972–84. [PubMed: 15021885]
16. Burger AM, Gao Y, Amemiya Y, et al. A novel RING-type ubiquitin ligase breast cancer-associated gene 2 correlates with outcome in invasive breast cancer. Cancer Res 2005;65:10401–12. [PubMed: 16288031]
17. Dornan D, Wertz I, Shimizu H, et al. The ubiquitin ligase COP1 is a critical negative regulator of p53. Nature 2004;429:86–92. [PubMed: 15103385]
18. Burger A, Li H, Zhang XK, et al. Breast cancer genome anatomy: correlation of morphological changes in breast carcinomas with expression of the novel gene product Di12. Oncogene 1998;16:327–33. [PubMed: 9467958]
19. Lipkowitz S. The role of the ubiquitination-proteasome pathway in breast cancer: ubiquitin mediated degradation of growth factor receptors in the pathogenesis and treatment of cancer. Breast Cancer Res 2003;5:8–15. [PubMed: 12559039]
20. Ohta T, Fukuda M. Ubiquitin and breast cancer. Oncogene 2004;23:2079–88. [PubMed: 15021895]
21. Connor MK, Azmi PB, Subramaniam V, Li H, Seth AK. Molecular characterization of ring finger protein 11. Mol Cancer Res 2005;3:453–61. [PubMed: 16123141]
22. Burger A, Amemiya Y, Kitching R, Seth AK. Novel RING E3 ubiquitin ligases in breast cancer. Neoplasia 2006;8:689–95. [PubMed: 16925951]
23. Mizuno K, Kitamura A, Sasaki T. Rabring7, a novel Rab7 target protein with a RING finger motif. Mol Biol Cell 2003;14:3741–52. [PubMed: 12972561]
24. Sakane A, Hatakeyama S, Sasaki T. Involvement of Rabring7 in EGF receptor degradation as an E3 ligase. Biochem Biophys Res Commun 2007;357:1058–64. [PubMed: 17462600]
25. Hook SS, Orian A, Cowley SM, Eisenman RN. Histone deacetylase 6 binds polyubiquitin through its zinc finger (PAZ domain) and copurifies with deubiquitinating enzymes. Proc Natl Acad Sci USA 2002;99:13425–30. [PubMed: 12354939]
26. Alam SL, Sun J, Payne M, et al. Ubiquitin interactions of NZF zinc fingers. EMBO J 2004;23:1411–21. [PubMed: 15029239]
27. Bienko M, Green CM, Crosetto N, et al. Ubiquitin-binding domains in Y-family polymerases regulate translesion synthesis. Science 2005;310:1821–24. [PubMed: 16357261]
28. Lee S, Tsai YC, Mattera R, et al. Structural basis for ubiquitin recognition and autoubiquitination by Rabex-5. Nat Struct Mol Biol 2006;13:264–71. [PubMed: 16462746]
29. Schnell JD, Hicke L. Non-traditional functions of ubiquitin and ubiquitin-binding proteins. J Biol Chem 2003;278:35857–60. [PubMed: 12860974]

30. Hurley JH, Lee S, Prag G. Ubiquitin-binding domains. Biochem J 2006;399:361–72. [PubMed: 17034365]

31. Yang Y, Yu X. Regulation of apoptosis: the ubiquitous way. FASEB J 2003;17:790–99. [PubMed: 12724336]

32. Lamothe B, Webster WK, Gopinathan A, Besse A, Campos AD, Darnay BG. TRAF6 ubiquitin ligase is essential for RANKL signaling and osteoclast differentiation. Biochem Biophys Res Commun 2007;359:1044–9. [PubMed: 17572386]

33. Burger AM, Salesiotis A, Panayiotakis A, Li H, Seth AK. Identification of differentially expressed genes in breast cancer. Int J Oncol 1996;8:395–400.

34. Garrus JE, von Schwedler UK, Pornillos OW, et al. Tsg101 and the vacuolar protein sorting pathway are essential for HIV-1 budding. Cell 2001;107:55–65. [PubMed: 11595185]

35. Trempe JF, Brown NR, Lowe ED, et al. Mechanism of Lys48-linked polyubiquitin chain recognition by the Mud1 UBA domain. EMBO J 2005;24:3178–89. [PubMed: 16138082]

36. Fisher RD, Wang B, Alam SL, et al. Structure and ubiquitin binding of the ubiquitin-interacting motif. J Biol Chem 2003;278:28976–84. [PubMed: 12750381]

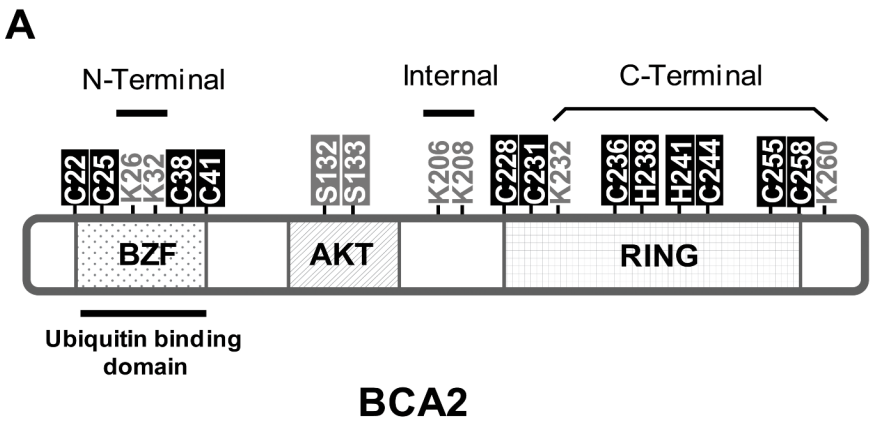

B

Accession#	Insert(kb)	Clone/ORF(aa)	Gene name
NP_066289	0.5-1.8	85-480/685	Polyubiquitin C
NM_003333	2.8	128/128	Ubiquitin-52 amino acid fusion protein (UBA52)
NM_003345	1.2	158/158	Ubiquitin-conjugating enzyme E2 (Ubc9)
NM_000980	0.6	176/176	60S ribosomal protein L18A

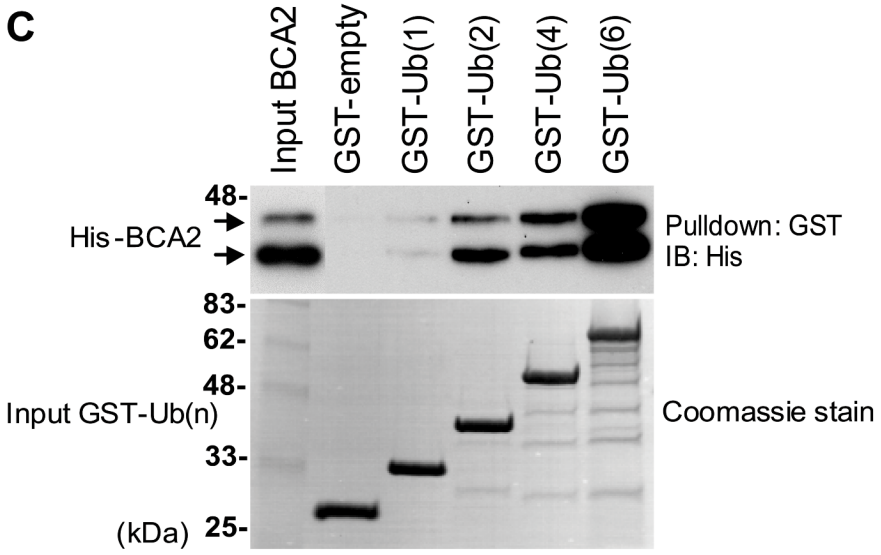

Figure 1.

A) Schematic diagram of BCA2. The position of the six lysine residues, K26 and K32 (N-terminal lysines), K206 and K208 (internal lysines) and K232 and K260 (C-terminal lysines), are shown as gray letters. Conserved cysteine (C22, C25, C38 and C41) residues in the BCA2 zinc finger (BZF), which we show is the functional ubiquitin binding domain and cysteine and histidine (C228, C231, C236, H238, H241, C244, C255 and C258) residues in the RING domain are shown on black background. The AKT phosphorylation sites (S132 and S133) are shown on gray background. B) Gene names and accession numbers of positive clones recovered from the bacterial two-hybrid tertiary screen of a human fetal brain library with the BCA2 wild type protein as bait are shown. C) Recombinant BCA2 binds ubiquitin. GST-Ub(n) (1, 2, 4, or

6 ubiquitin tandem repeats) immobilized on glutathione sepharose beads were incubated with recombinant His-tagged BCA2. The pulldowns were immunoblotted with anti-His antibody (upper panel). The coomassie brilliant blue R-250 staining of SDS-PAGE gel shows the amount of GST-Ub(n) fusion proteins used in each pulldown assay (lower panel).

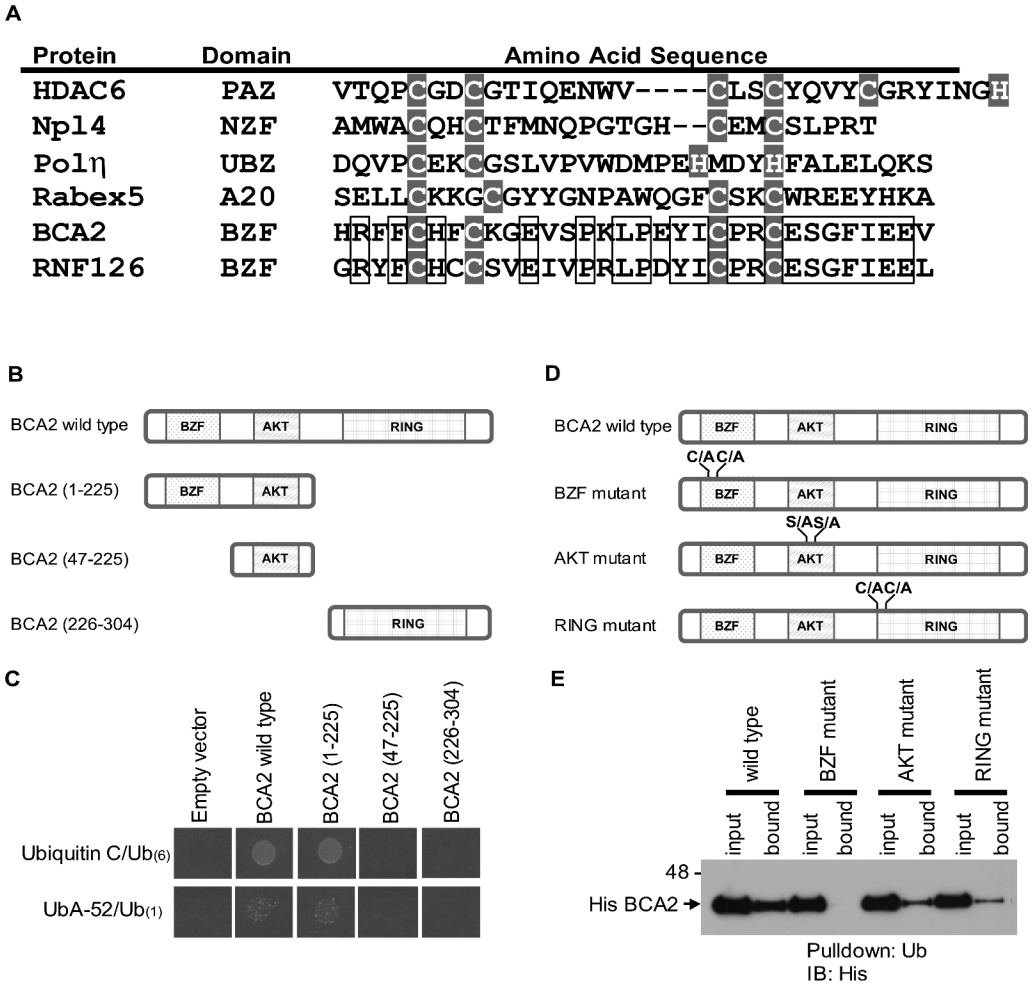

Figure 2.

BCA2 interacts with ubiquitin via BZF domain. (A) Sequence comparison of the BZF domain and various zinc finger type ubiquitin binding domains. Amino acid sequence were taken from PAZ (25), NZF (26), UBZ (27) and A20 (28). Gray shaded letters denote conserved cysteine and histidine residues for zinc finger domains. Open boxes show conserved amino acids within BZF domains of BCA2 and RNF126. A dash indicates a gap inserted to maximize conserved amino-acid alignment. (B) Schematic diagram of BCA2 and its deletion mutants used for directed bacterial two hybrid assay. (C) Bacterial cells expressing the BCA2 wild type or N-terminal fragment (1-225) of BCA2 interact with both 6 tandem ubiquitin and UbA-52 ribosomal fusion protein grown in selective plate containing 3-AT and streptomycin while pBT empty vector, BCA2 internal fragment (47-225) and C-terminal fragment (226-304) failed to interact with Ubiquitin. (D) Schematic diagram of BCA2 and its point mutants used for pull down assay in (E). (E) Recombinant his-tagged BCA2 and its BZF, AKT and RING mutants were subjected to pull-down assays with GST-Ub(4) immobilized on glutathione sepharose beads. GST-Ub(4) bound to BCA2 wild type, AKT and RING mutants but not to BCA2 BZF mutant.

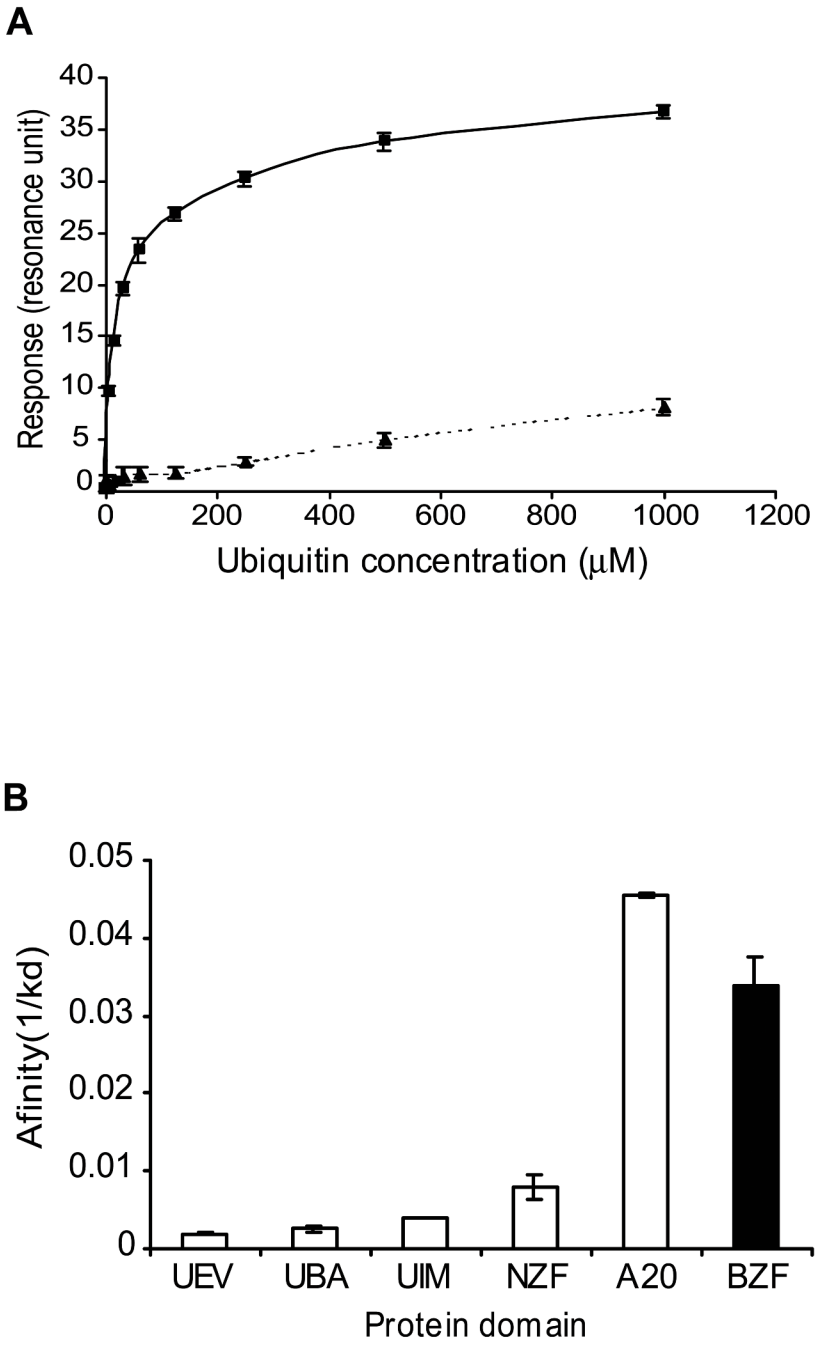

Figure 3.

Quantification of BZF domain affinity for ubiquitin. (A) Determination of the dissociation constant by measuring the amount of ubiquitin bound to BZF domain of BCA2 using SPR. Ubiquitin protein was injected in triplicate at concentrations of 0-1000 mM over His tagged BCA2 immobilized on CM5 sensor chip (squares, Kd = 29.6+/-3.2mM). Much weaker binding (Kd) response was obtained when the same concentrations of ubiquitin was injected over BCA2 treated with zinc ejecting compound, disulfiram (triangles with dotted line). Fitted curves are shown. Error bars indicate standard deviation based on three independent experiments. (B) Comparison of binding affinity of BCA2-BZF domain and various distinct ubiquitin binding

domains, UEV (34), UBA (35), UIM (36), NZF (26) and A20 (28) All binding affinities were measured by SPR.

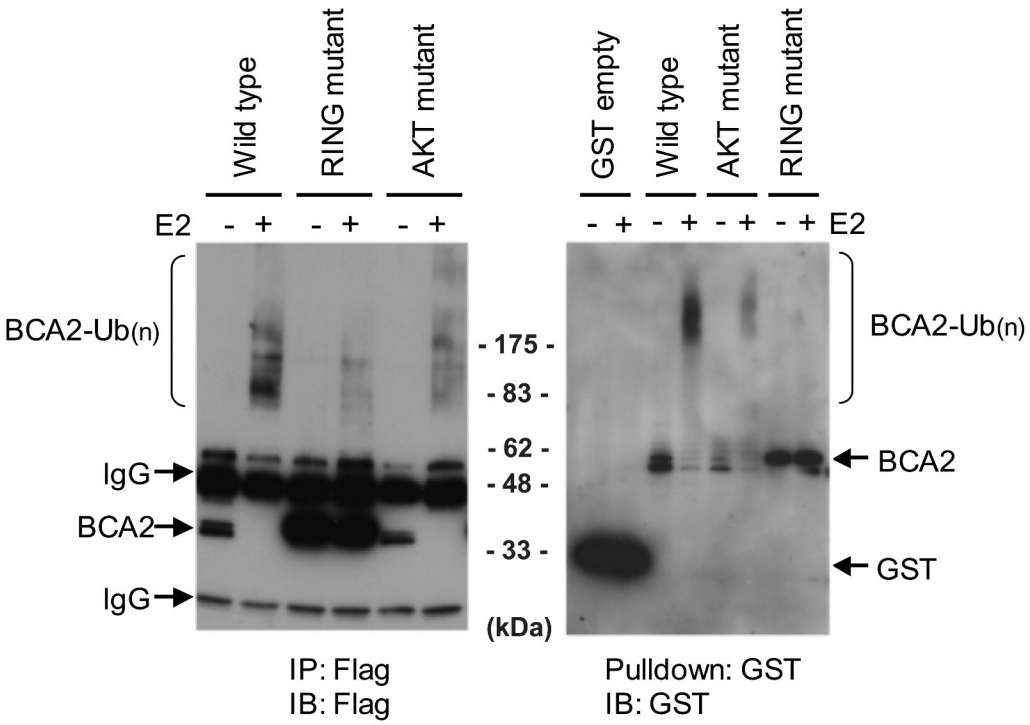

Figure 4.

Autoubiquitination of the BCA2 proteins. BCA2 and its mutants as indicated above each lane were expressed using the pCMV-tag2B-Flag vector or pEBG-GST vector in HEK293T cells. Flag-tagged proteins were immunoprecipitated (IP) with monoclonal anti-Flag antibodies and incubated with protein A sepharose beads. GST-tagged proteins were pull-downed with Glutathione Sephaose 4B. Washed beads were incubated with ubiquitin, ATP, mouse E1, and with (+) or without (-) the bacterial E2 UbcH5b. Left panel shows anti-Flag immunoblot of autoubiquitination assay for Flag-tagged BCA2. Right panel shows anti-GST immunoblot of autoubiquitination assay for GST-tagged BCA2.

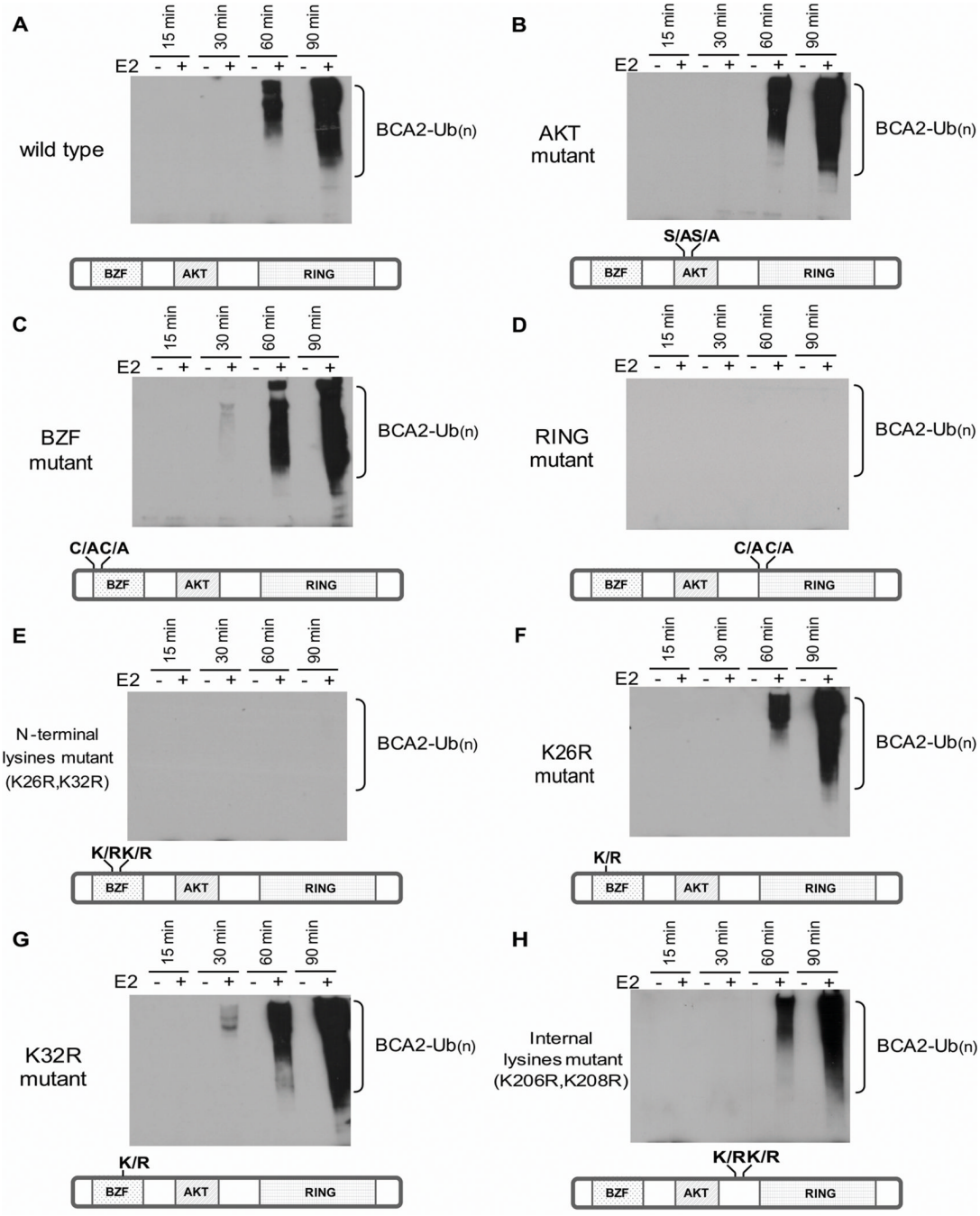

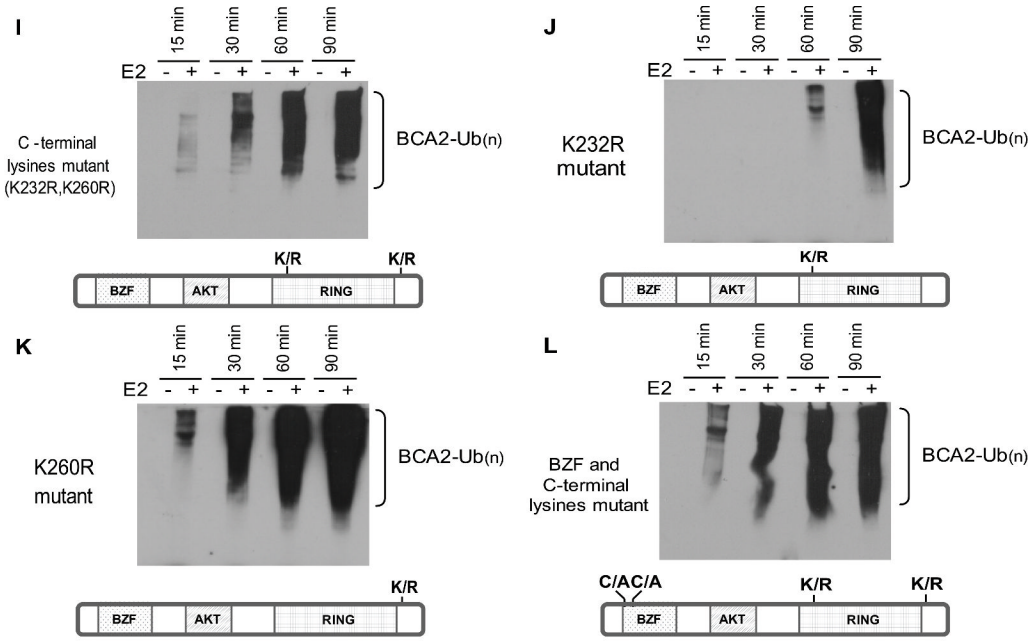

Figure 5.

Time course for the detection of BCA2 and its mutants autoubiquitination. Time course of in vitro ubiquitination reactions (15 min, 30 min, 60 min and 90 min) conducted in the presence (+) or absence (-) of bacterial extract containing the E2-conjugating enzyme UbcH5b and purified ubiquitin with E1 protein, using bacterially expressed (A) His-BCA2, (B) His-BCA2 AKT mutant, (C) His-BCA2 BZF mutant, (D) His-BCA2 Ring mutant, (E) His-BCA2 N-terminal lysine (K26R, K32R) mutant, (F) His-BCA2 K26R mutant, (G) His-BCA2 K32R, (H) His-BCA2 internal lysine (K206R, K208R) mutant, (I) His-BCA2 C-terminal (K232R, K260R) mutant, (J) His-BCA2 K232R mutant, (K) His-BCA2 K260R mutant, (L) and His-BCA2 BZF + C-terminal (K232R, K260R) mutant. Autouiquitination assay conditions are described in Material and Methods

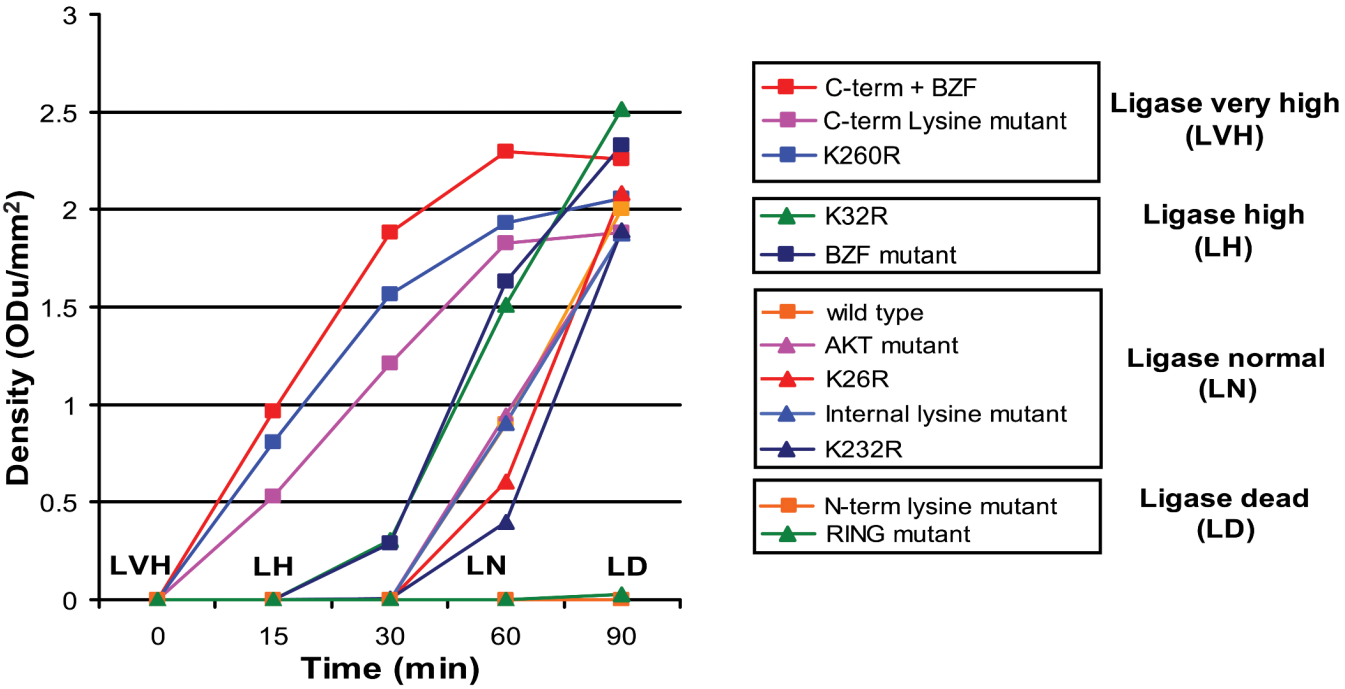

Figure 6.

Comparison of E3 ligase activity of BCA2 and its mutants. The optical density (OD) of individual band of each Western blot (Fig. 6 A - L) was quantitated using the Quantity One software (ver. 4.3.1, Bio-Rad Laboratories, Segrate, Milan, Italy) and normalized by subtracting the OD of an area of identical size from the blank lane of the each gel.

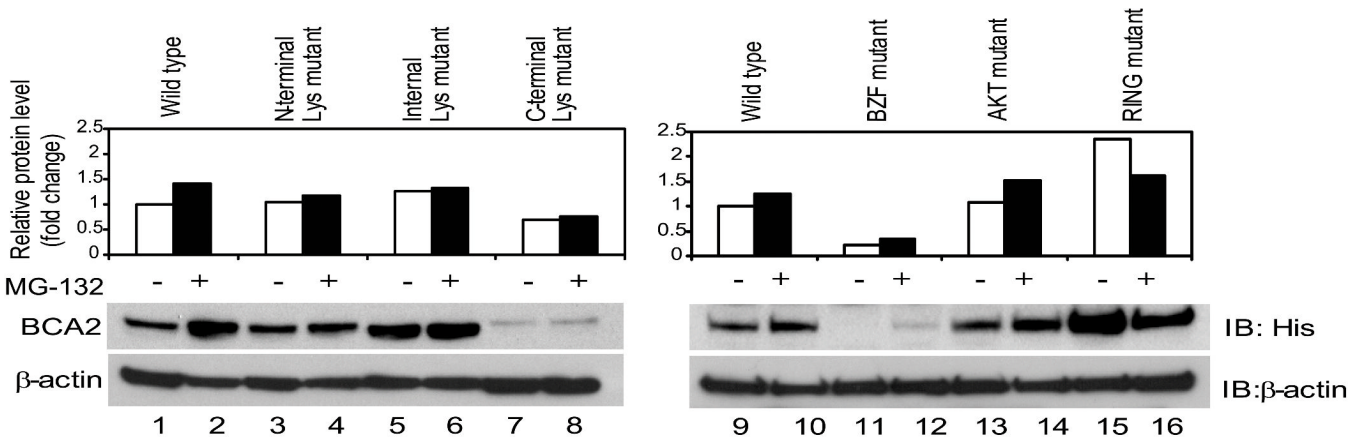

Figure 7.

Stability of transiently expressed BCA2 wild type and its mutants. Equal amounts of His-tagged BCA2 wild type and its mutant vector DNA were transfected into HEK293T cells. The total transfection period was 48 hours. 10mM of MG-132 (+) or DMSO (-) were added 40 hours after transfection, resulting in drug exposure of 8 hours. Whole cell lysate were immunoblotted with anti-His (upper panel) or β-actin was used as a loading control (lower panel). Bar graph shows normalized fold protein level of BCA2 and its mutants relative to BCA2 wild type MG-132 (-) using β-actin as internal control.

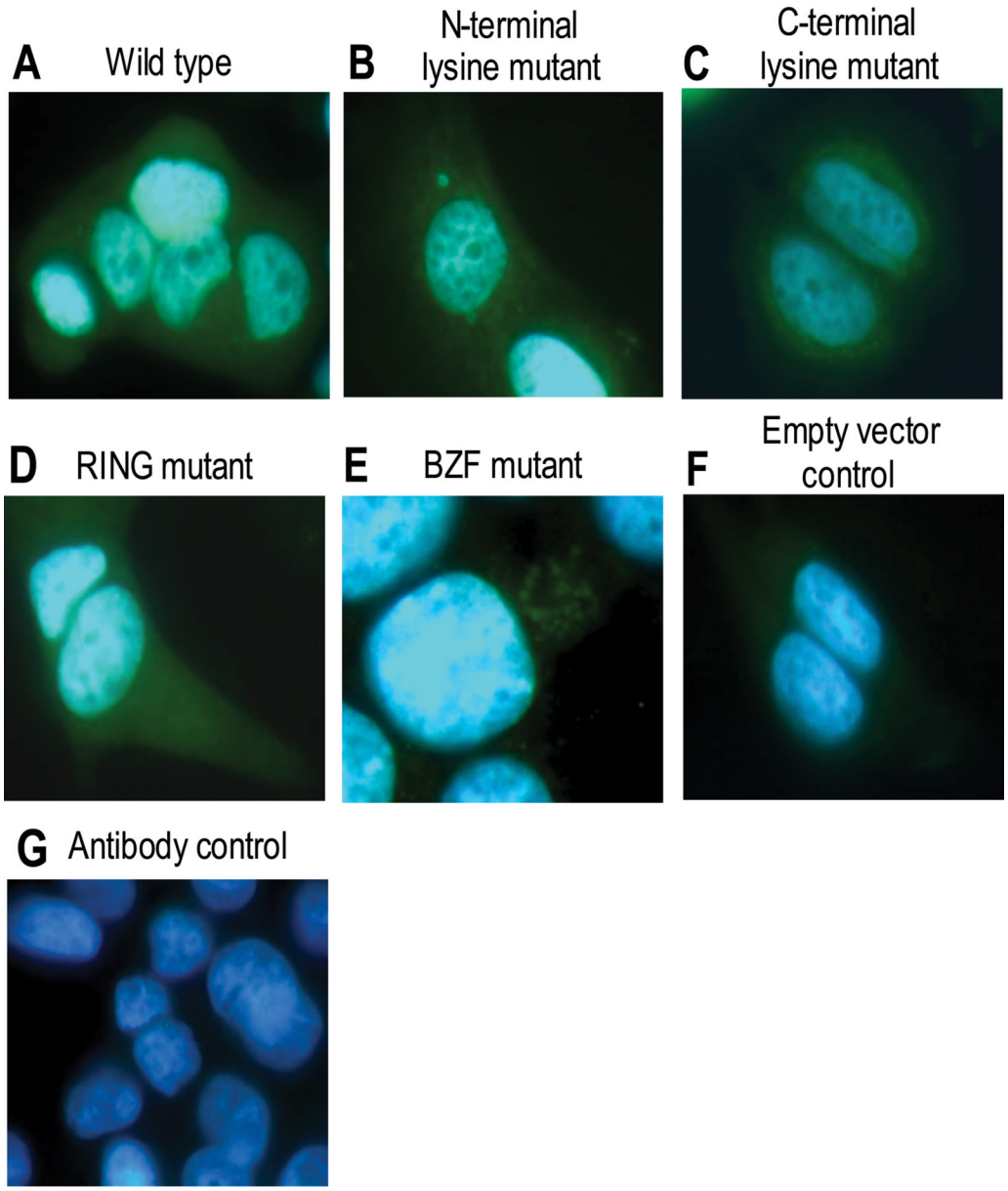

Figure 8.

BCA2 and its variants expression in MCF7 cells. MCF7 cell lines that stably express BCA2 or selected mutant variants were examined by immunofluorescence as described in Material and Methods. Fixed cells were probed with the monoclonal anti-polyhistidine (AD1.1.10) antibody for 8 hours followed by anti-mouse FITC-secondary fluorescent antibody. Cell nuclei were stained with DAPI. In situ immunoflourecence reveals different expression patterns for the BCA2 protein variants. (A) MCF7 cells expressing BCA2 wild type protein. (B) MCF7 cells expressing BCA2 N-terminal lysine mutant protein. (C) MCF7 cells expressing BCA2 C-terminal lysine mutant protein. (D) MCF7 cells expressing BCA2 RING mutant protein. (E) MCF7 cells expressing BCA2 BZF mutant protein. (F) MCF7 cells expressing His tag alone (Empty vector). (G) Negative control in which only secondary FITC antibody was incubated with MCF7 cells expressing the His tag from the empty vector.

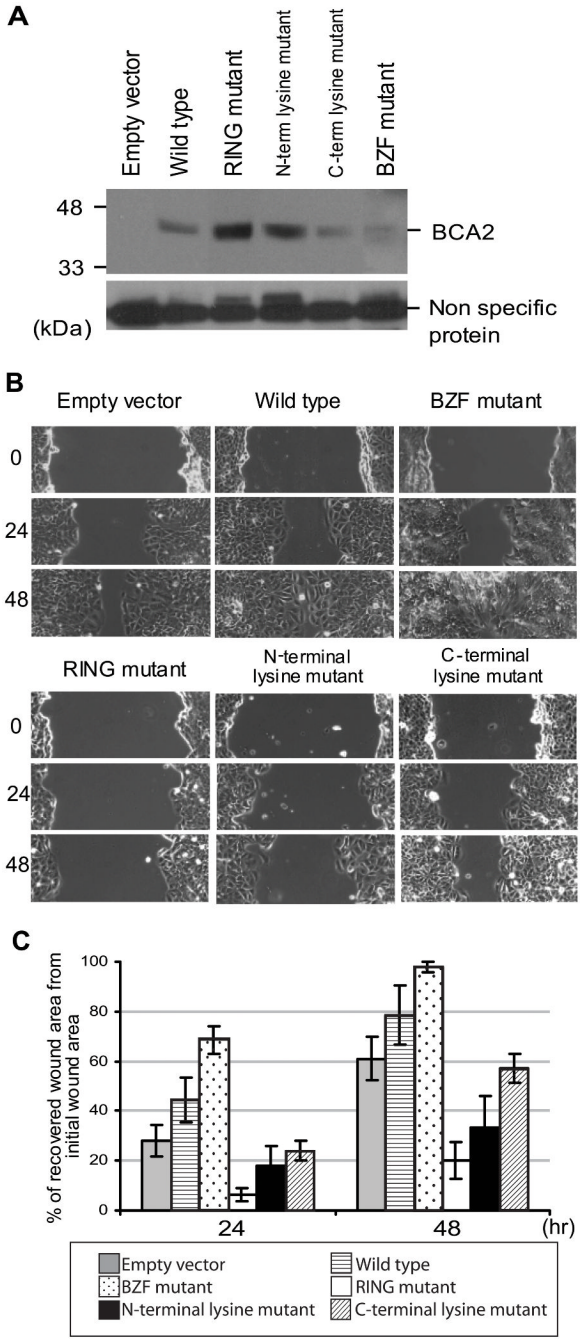

Figure 9.

Effects of BCA2 and mutants on MCF7 cell migration. (A) anti-His immunoblot of MCF7 cells stably transfected with pEF1-His-BCA2 wild type and its mutants (upper panel). Non-specific band obtained by anti-His was used as a loading control (lower panel). (B) MCF7 cells stably expressing BCA2 or its mutants were serum starved for 18 h, scratched with a sterile pipette tip, and treated with DMEM medium containing 10% FBS and 10mM Hydroxyurea. Cells were allowed to migrate into the denuded area, and phase micrographs taken at 0, 24, and 48 h. (C) Graph shows the percentage of recovered wound area from the initial wound area after 24 and 48 h of migration. Error bars indicate S.D. based on three independent experiments.

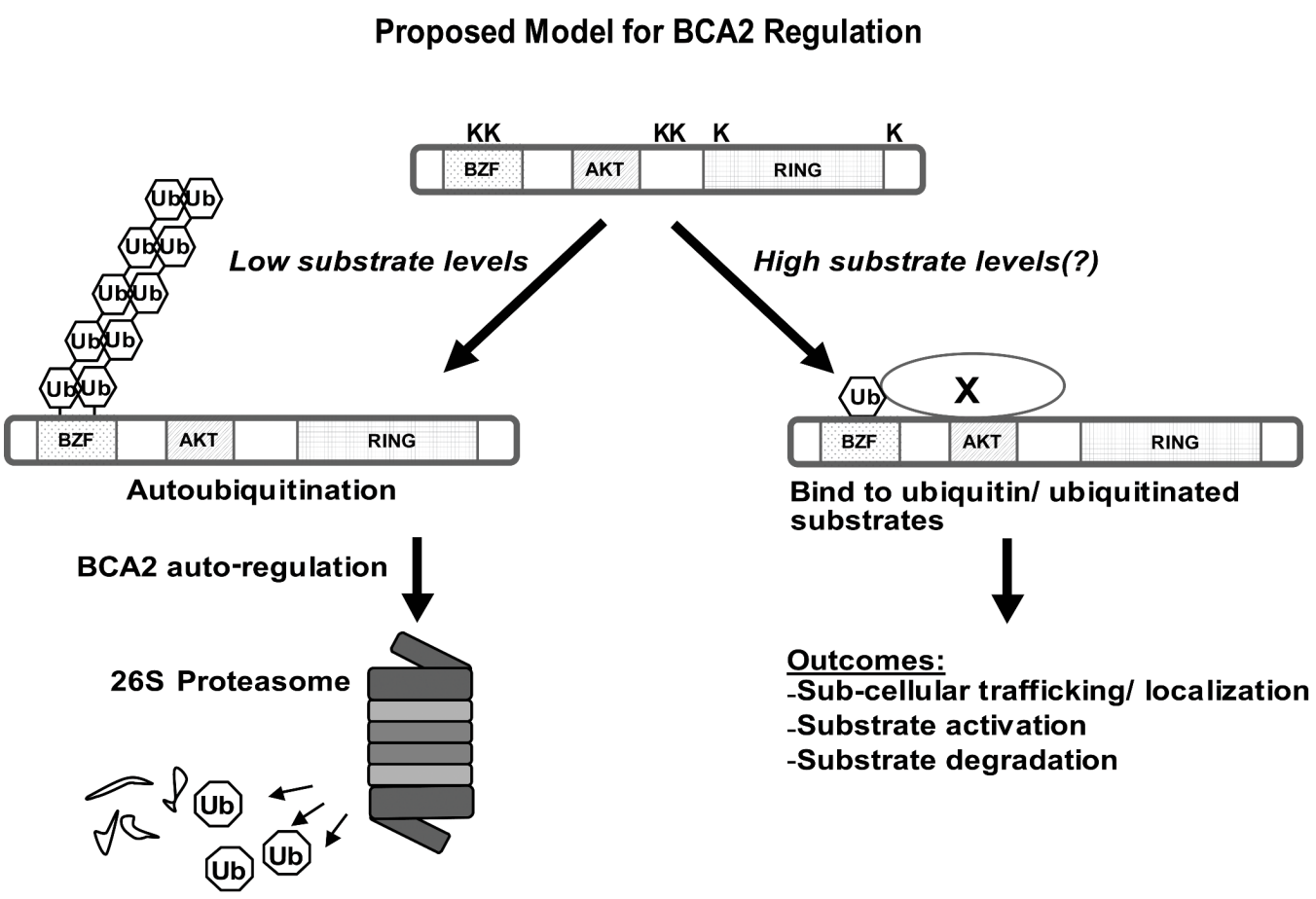

Figure 10.
Proposed Model for BCA2 Regulation